Featured in Physics

Compressed Ultrafast Spectral-Temporal Photography

Yu Lu,[1,2] Terence T. W. Wong,[3] Feng Chen,[1,*] and Lidai Wang[2,4,†]

[1]*State Key Laboratory for Manufacturing System Engineering and Key Laboratory of Photonics Technology for Information of Shaanxi Province, School of Electronics & Information Engineering, Xi'an Jiaotong University, 28 Xianning West Road, Xi'an, Shaanxi 710049, China*

[2]*Department of Biomedical Engineering, City University of Hong Kong, 83 Tat Chee Ave, Kowloon, Hong Kong SAR, China*

[3]*Translation and Advanced Bioimaging Laboratory, Department of Chemical and Biological Engineering, Hong Kong University of Science and Technology, Clear Water Bay, Kowloon, Hong Kong SAR, China*

[4]*City University of Hong Kong Shenzhen Research Institute, Yuexing Yi Dao, Nanshan District, Shenzhen, Guang Dong, 518057, China*

(Received 16 November 2018; revised manuscript received 18 March 2019; published 17 May 2019)

Acquiring ultrafast and high spectral resolution optical images is key to measure transient physical or chemical processes, such as photon propagation, plasma dynamics, and femtosecond chemical reactions. At a trillion Hz frame rate, most ultrafast imaging modalities can acquire only a limited number of frames. Here, we present a compressed ultrafast spectral-temporal (CUST) photographic technique, enabling both an ultrahigh frame rate of 3.85 trillion Hz and a large frame number. We demonstrate that CUST photography records 60 frames, enabling precisely recording light propagation, reflection, and self-focusing in nonlinear media over 30 ps. CUST photography has the potential to further increase the frame number beyond hundreds of frames. Using spectral-temporal coupling, CUST photography can record multiple frames with a subnanometer spectral resolution with a single laser exposure, enabling ultrafast spectral imaging. CUST photography with high frame rate, high spectral resolution, and high frame number in a single modality offer a new tool for observing many transient phenomena with high temporal complexity and high spectral precision.

DOI: 10.1103/PhysRevLett.122.193904

Introduction.—Ultrafast photography is a major driving technique to extend our understanding of transient processes. For example, the pump-probe technique, initialized by Zewail in the 1980s, acquires single-snapshot ultrafast graphic or spectral information with a temporal resolution of femtoseconds or even attoseconds [1–5]. However, the pump-probe method relies on multiple measurements with different time delays between the pump and the probe and can be applied to only repeatable processes. Measuring ultrafast and nonrepeatable phenomena, such as laser surgery [6,7], exciton diffusion [8], or laser-bio-tissue interaction [9,10], motivates the development of single-shot ultrafast imaging technology. Recently, several single-shot ultrafast photography techniques have been developed, such as serial time-encoded amplified imaging (STEAM) [11–13], compressed ultrafast photography (CUP) [14,15], sequentially timed all-optical mapping photography (STAMP) [16–18], and frequency recognition algorithm for multiple exposures (FRAME) [19]. However, due to the limitation of pulse width or pulse repetition rate, speed of the imaging sensors, or the image reconstruction methods, compromise among imaging speed, spectral resolution, and frame number remains a challenge in ultrafast photography.

Here, we present compressed ultrafast spectral-temporal (CUST) photography, offering a 3.85-trillion-Hz frame rate, a subnanometer spectral resolution, and a large frame number. In a single laser shot, over 60 frames can be captured with either 100-fs frame interval or sub-nm spectral resolution. The temporal or spectral information is spatially encoded and compressed into a single 2D image. Multiple temporally or spectrally resolved images are reconstructed from the compressed 2D image using a compressed sensing algorithm [20–23]. The reconstructed images are not limited by the speed of the imaging sensor, ensuring a large frame number with a high temporal or spectral resolution. We demonstrate the feasibility to record transient, highly complex and nonrepetitive events, breaking through the limit of large-frame-number recording with an ultrahigh temporal or spectral resolution.

Principle.—The principle of CUST photography is shown in Fig. 1 (the detailed principle is presented in the Supplemental Material [24], Appendix). The CUST system consists of three modules, spectral-shaping module (SSM), pulse-stretching module (PSM), and compressed camera. In the SSM, an fs laser pulse (pulse width, 50 fs; central wavelength, 800 nm; bandwidth, 18 nm) passes through a pair of gratings (1200 lines/mm@750 nm) and a 4F system. The SSM selects a designated spectrum of the fs pulse via tuning a slit in the Fourier plane of the 4F system. The SSM can also be used to calibrate the CUST photography system (see details in the Supplemental Material [24], Appendix). In the PSM, the fs pulse is stretched by another

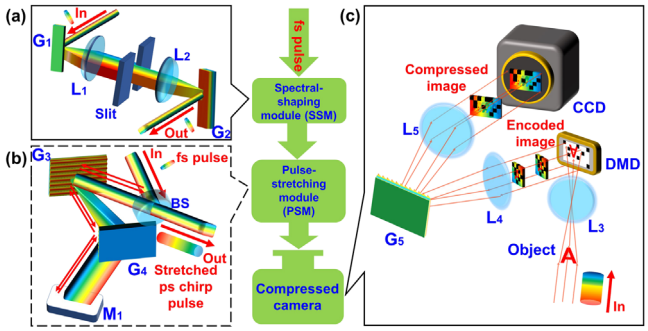

FIG. 1. Principle of compressed ultrafast spectral-temporal photography. (a) Spectral-shaping module selects wavelengths for imaging. (b) Pulse-stretching module stretches the fs laser pulse to the full imaging time. (c) Compressed camera: a DMD encodes the laser beam with a pseudo-random binary pattern. A grating disperses the encoded graphs spatially by different wavelengths. A CCD sensor records the compressed 2D image. Caption: beam splitter (BS).

grating pair (1200 lines/mm@750 nm). The spatial-temporal distribution of the stretched pulse is denoted as a density matrix $\mathbf{I}$. At the scene plane, the stretched pulse transmits through an ultrafast object $O(x, y, t)$. Then the light beam is projected on to a digital micro-mirror device (DMD) through an imaging lens [L_3 in Fig. 1(c)]. The DMD spatially encodes the light beam with a pseudorandom binary patterns $\mathbf{E}$, yielding an image S written as

$$S = \mathbf{E} \cdot \mathbf{I} \cdot O. \tag{1}$$

The encoded beam is further dispersed by a set of optics [L_4, G_5, and L_5 in Fig. 1(c)]. The lenses L_4 and L_5 form a 4F system. The grating G_5 is placed on the Fourier plane of the 4F system. The dispersed beam is received by a CCD sensor. The recorded image $F(x, y)$ can be written as

$$F(x, y) = \mathbf{T} \cdot S = \mathbf{T} \cdot \mathbf{E} \cdot \mathbf{I} \cdot O = \mathbf{C} \cdot O(x, y, t), \tag{2}$$

where the 4F system and the grating G_5 are mathematically denoted as a transfer matrix $\mathbf{T}$, $\mathbf{C}$ is a transform matrix. By opening a narrow slit (50-μm width) in the frequency plane of SSM module and successively moving the slit along it, the transform matrix $\mathbf{C}$ can be precalibrated (see Supplemental Material [24], Appendix). The dimension of $F(x, y)$ is much lower than that of vector $O(x, y, t)$. If matrix $\mathbf{E}$ is a pseudorandom binary pattern and $O(x, y, t)$ is spatially sparse, we can reconstruct the $O(x, y, t)$ from $F(x, y)$ with a compressed sensing algorithm. In this Letter, we adopt a two-step iterative shrinkage or thresholding (TwIST) algorithm to reconstruct the ultrafast object [20].

Results.—Ultrafast imaging: To demonstrate the imaging speed of CUST photography, transient light propagation is recorded. In the experiments, an fs pulsed light beam incidents into a CS_2 medium and is recorded based on optical Kerr gate (OKG) effect [25,26]. Three straightly propagating light pulses are shown in Fig. 2(a) with a frame interval of 260 fs. Figure 2(a) shows one snapshot every five recorded frames, and the time interval between two adjacent snapshots is 1.302 ps. Images show that the light pulses gradually move with a step size of ~250 μm every snapshot (five frames), i.e., ~50 μm per frame. Supplemental Material, video_S1 [24] shows the entire light propagation process with a temporal interval of 260 fs for 40 frames. The trajectories of the pulse centers in Fig. 2(a) have been shown in Fig. 2(b) with different colors. As shown in Fig. 2(b), the light pulse centers move approximately along straight lines. With different straight lines, the standard deviations of spot centers are 5.5 (green line), 8.2 (blue line), and 15.6 μm (red line). Wobbles of light spot centers to the fitted lines are evident, which originates from the deviations brought by compression and reconstruction processes. Figure 2(c) and a Supplemental Material [24] (video_S2) show the light reflection recorded with a frame interval of 414 fs for 60 frames. In Fig. 2(c), we plot one snapshot every six frames. Compared with the results in Fig. 2(a), the light reflection recording covers a longer light-fight time, a longer frame interval and more frames. After 19.872 ps, the light spot size decreases below 0.5 mm. When the laser beam propagates, high intensity in the beam center may induce a higher refractive index than that in the surrounding region. As a result, the self-focusing and beam divergence reach an equilibrium, and the reflected beam remains the same size.

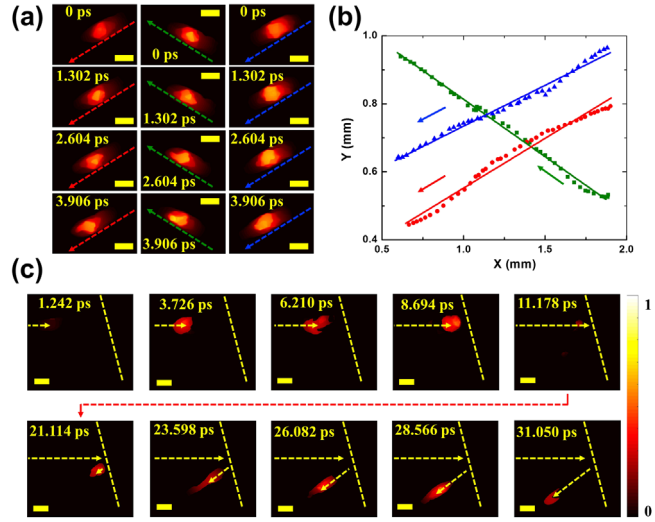

FIG. 2. Ultrafast imaging of light propagation. (a) Three sets of temporal snapshots of flying light pulse. (b) Estimated trajectories of light pulse centers. (c) Snapshots of reflected light pulse. Total frame number, 60; frame interval, 414 fs. The arrows show the light propagation direction. The yellow dashed line presents the boundary of Kerr gate medium (CS_2). A reflecting mirror is placed out of the medium container with a small gap. The photons outside of the CS_2 medium are not recorded due to the absence of the Kerr gate effect. Scale bars: 0.5 mm.

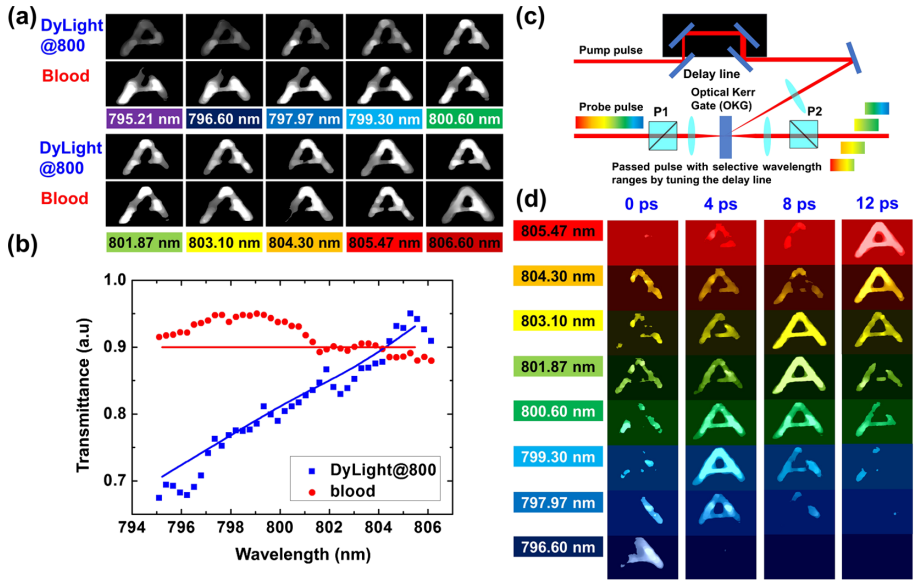

FIG. 3. Single-shot spectral image. (a) Spectral imaging of near-infrared dye DyLight@800 and blood samples from 795.21 to 806.60 nm. (b) Average transmittances of power meter (solid lines) measurements and CUST spectral images (scattered points). (c) Principle of ultrafast spectral imaging in a spectral tailoring system. Illumination spectrum is selected via tuning the time delay between the pump and probe pulses generated by the (pulse stretching module) PSM. (d) Four sets of single-shot spectral images with central wavelengths from 796.60 to 805.47 nm. Each column is acquired with one laser exposure. The time delays for the four sets of spectral images change from 4 to 20 ps.

Ultrafast spectral photography.—The spectral imaging capability of CUST photography is demonstrated in Fig. 3. Near-infrared dye DyLight@800 (Thermo Fisher Scientific Inc.) and 100% oxygenated blood samples are deposited into pattern "*A*." Within a spectrum from 795.21 to 806.60 nm, 46 frames are recorded with a spectral resolution of 0.25 nm. In this wavelength range, the extinction coefficient of DyLight@800 dye can decreases by 28% with wavelength increasing, but oxygenated blood's extinction coefficient only decreases by 8% [27]. The spectral imaging experiment results show transmittances agreeing with the spectra of the two absorbers. In Fig. 3(a), the transmission image of near-infrared dye DyLight@800 shows a clear trend from dark to bright as the wavelength increases. In contrast, the brightness of the blood sample image does not show obvious changes with wavelength. The difference between the transmission spectra of DyLight@800 and oxygenated hemoglobin is also validated by the transmittances measured by both CUST photography and a power meter in Fig. 3(b). The transmittance was measured by averaging all the signals in CUST images, which was compared with the power meter measurements. The transmittance of DyLight@800 increases from 0.67 to 0.93 as wavelength changes from 795.21 to 806.60 nm. The transmission spectrum of blood remains almost the same as the wavelength changes.

Ultrafast spectral imaging is demonstrated in Figs. 3(c) and 3(d). Figure 3(c) shows the principle of the ultrafast spectral imaging. A chirped pulse is tailored with an OKG. The selected spectrum illuminates an object (pattern *A*) to generate spectral images. The spectral images are encoded, compressed and recorded by CUST, and then reconstructed with the compressed sensing algorithm. Via tuning the time delay of a pump beam from 0 to 12 ps, the OKG can select a different central wavelength of the spectrum. Figure 3(d) shows different groups of spectral images acquired at four different time delays. When the time delay is 0 ps, the brightest image exists at a wavelength of 796.60 nm. As the time delay increases to 4, 8, and 12 ps, the brightest images shift to 799.30, 803.10, and 805.47 nm, respectively. In the chirped pulse, the short wavelength components arrive at the OKG earlier than the longer ones. As a result, short wavelengths are selected by OKG first with a short time delay, and long wavelengths pass the OKG with an increased time delay. With this ultrafast spectral imaging technique, we can capture tens of spatial and spectral images simultaneously within an ~ps timescale.

Conclusions.—In conclusion, CUST photography can image ultrafast processes with an fs-scale speed and a large frame number. We demonstrate imaging of light propagation with 3.85 trillion Hz frame rate for 60 frames. CUST enables us to visualize the self-focusing phenomenon with abundant temporal and spatial details. CUST can also acquire multiple spectrally resolved images with one laser exposure. Using our femtosecond laser, CUST can acquire 60 spectral images with 0.25-nm spectral resolution within ~ps timescale.

A major advantage of CUST is the large frame number and high temporal or spectral resolution in a single modality. In addition, the imaging speed can be adjusted, which gives CUST extra advantage. For example, via

tuning the incident angle of the grating pair in the pulse stretching module (SSM), the temporal resolution of CUST can be continuously tuned from 0.1 to 5 ps.

CUST uses a chirped pulse to illuminate the ultrafast process. Thus, it is challenging for CUST to image self-illuminating processes such as fluorescence processes. Because CUST uses a compressed sensing algorithm in image reconstruction, the reconstructed image quality may not be optimal compared with other direct imaging methods. The compressed sensing method needs further optimization to image the imaging quality.

This work is partially supported by Research Grants Council of the Hong Kong Special Administrative Region (ECS 21205016 and GRF 11215817); City University of Hong Kong startup grant (9610339); National Natural Science Foundation of China (NSFC) (81627805), (51335008), and (61475124).

*Corresponding authors.
chenfeng@mail.xjtu.edu.cn
†Corresponding authors.
lidawang@cityu.edu.hk

[1] A. H. Zewail, J. Phys. Chem. A **104**, 5660 (2000).
[2] P. B. Corkum and F. Krausz, Nat. Phys. **3**, 381 (2007).
[3] M. T. Hassan, T. T. Luu, A. Moulet, O. Raskazovskaya, P. Zhokhov, M. Garg, N. Karpowicz, A. M. Zheltikov, V. Pervak, F. Krausz, and E. Goulielmakis, Nature (London) **530**, 66 (2016).
[4] M. Ulberacker, T. Uphues, M. Schultze, A. J. Verhoef, V. Yakovlev, M. F. Kling, J. Rausehenberger, N. M. Kabachnik, H. Schröder, M. Lezius, K. L. Kompa, H.-G. Muller, M. J. J. Vrakkinig, S. Hendel, U. Kleineberg, U. Heinzmann, M. Drescher, and F. Krausz, Nature (London) **446**, 627 (2007).
[5] H. Hou, X. Mao, V. Zorba, and R. E. Russo, Anal. Chem. **89**, 7750 (2017).
[6] C. Samara, C. B. Rohde, C. L. Gilleland, S. Norton, S. J. Haggarty, and M. F. Yanik, Proc. Natl. Acad. Sci. U.S.A. **107**, 18342 (2010).
[7] A. Vogel, N. Linz, S. Freidank, and G. Paltauf, Phys. Rev. Lett. **100**, 038102 (2008).
[8] O. V. Kozlov, F. De Haan, R. A. Kerner, B. P. Rand, D. Cheyns, and M. S. Pshenichnikov, Phys. Rev. Lett. **116**, 057402 (2016).
[9] K. Sugioka and Y. Cheng, Light Sci. Appl. **3**, e149 (2014).
[10] C. Kerse, H. Kalaycloğ Lu, P. Elahi, B. Çetin, D. K. Kesim, Ö. Akçaalan, S. Yavaş, M. D. Aşlk, B. Öktem, H. Hoogland, R. Holzwarth, and F. Ö. Ilday, Nature (London) **537**, 84 (2016).
[11] K. Goda, K. K. Tsia, and B. Jalali, Nature (London) **458**, 1145 (2009).
[12] K. Goda, A. Ayazi, D. R. Gossett, J. Sadasivam, C. K. Lonappan, E. Sollier, A. M. Fard, S. C. Hur, J. Adam, C. Murray, C. Wang, N. Brackbill, D. Di Carlo, and B. Jalali, Proc. Natl. Acad. Sci. U.S.A. **109**, 11630 (2012).
[13] J.-L. Wu, Y.-Q. Xu, J.-J. Xu, X.-M. Wei, A. C. Chan, A. H. Tang, A. K. Lau, B. M. Chung, H. Cheung Shum, E. Y. Lam, K. K. Wong, and K. K. Tsia, Light Sci. Appl. **6**, e16196 (2017).
[14] L. Gao, J. Liang, C. Li, and L. V. Wang, Nature (London) **516**, 74 (2014).
[15] J. Liang, L. Zhu, and L. V. Wang, Light Sci. Appl. **7**, 42 (2018).
[16] T. Suzuki, F. Isa, L. Fujii, K. Hirosawa, K. Nakagawa, K. Goda, I. Sakuma, and F. Kannari, Opt. Express **23**, 30512 (2015).
[17] T. Suzuki, R. Hida, Y. Yamaguchi, K. Nakagawa, T. Saiki, and F. Kannari, Appl. Phys. Express **10**, 092502 (2017).
[18] M. Tamamitsu, K. Nakagawa, R. Horisaki, A. Iwasaki, Y. Oishi, A. Tsukamoto, F. Kannari, I. Sakuma, and K. Goda, Opt. Lett. **40**, 633 (2015).
[19] A. Ehn, J. Bood, Z. Li, E. Berrocal, M. Aldén, and E. Kristensson, Light Sci. Appl. **6**, e17045 (2017).
[20] M. A. T. Figueiredo, R. D. Nowak, and Stephen J. Wright, IEEE J. Sel. Top. Signal Process. **1**, 586 (2007).
[21] M. F. Duarte, M. A. Davenport, D. Takhar, J. N. Laska, T. Sun, K. F. Kelly, and R. G. Baraniuk, IEEE Signal Process. Mag. **25**, 83 (2008).
[22] G.-H. Chen, J. Tang, and S. Leng, Proc. SPIE-Int. Soc. Opt. Eng. **6856**, 685618 (2008).
[23] J. M. Bioucas-Dias and M. A. T. Figueiredo, IEEE Trans. Image Process. **16**, 2992 (2007).
[24] See Supplemental Material at http://link.aps.org/supplemental/10.1103/PhysRevLett.122.193904 for more details on (i) Appendix: Detailed mathematical description about CUST principle and technique details about system pre-calibration, (ii) Video_S1: A movie of straightly flying light pulse. 40 frames with 260 fs frame interval, (iii) Video_S2: A movie of a reflecting light pulse. 60 frames with 414 fs frame interval.
[25] L. Wang, P. P. Ho, C. Liu, G. Zhang, and R. R. Alfano, Science **253**, 769 (1991).
[26] X. Wang, J. Si, L. Yan, P. He, F. Chen, and X. Hou, J. Opt. **16**, 015203 (2014).
[27] J. Laufer, C. Elwell, D. Delpy, and P. Beard, Phys. Med. Biol. **50**, 4409 (2005).